

# Hard X-Ray Lightcurves of High Mass X-Ray Binaries

S. Laycock,<sup>1</sup> M. J. Coe,<sup>1</sup>

C.A. Wilson<sup>2</sup>, B. A. Harmon<sup>2</sup>, M. Finger,<sup>2</sup>

<sup>1</sup>*Department of Physics and Astronomy, Southampton University, SO17 1BJ, UK*

<sup>2</sup>*NASA, MSFC, Huntsville, AL35812, USA*

Accepted . Received ; in original form

## ABSTRACT

Using the 9 years of continuous data now available from the Burst And Transient Source Experiment (BATSE) aboard CGRO, we have measured orbital periods and produced folded lightcurves for 8 High Mass X-ray Binaries (HMXB). Given the length of the datasets, our determinations are based on many more binary orbits than previous investigations. Thus our source detections have high statistical significance and we are able to follow long-term trends in X-ray output. In particular we focus on two systems: A0538-668 and EXO2030+375 both HMXBs exhibiting Type I outbursts.

Recent work on A0538-668 (Alcock et al 1999) reported a 16.65d optical variability due to the orbital period, but only seen during minima of a longer-term variability at 421d. We searched for this signal in the BATSE dataset using an ephemeris derived from Alcock et al ( 1999) & Skinner ( 1982). We found no evidence for such modulation and place an upper limit of  $3.0 \times 10^{-3}$  photon  $\text{cm}^{-2} \text{s}^{-1}$  in the 20-70 keV BATSE energy band , based upon statistical modelling of the signal. Previous observations of EXO 2030+375 (Reig et al 1998) using RXTE ASM data indicate secondary outbursts occur at apastron passage. We present a lightcurve for an earlier epoch showing convincing evidence for such apastron outbursts. We find apastron outbursts in 3 sources, all having orbital periods greater than 41d. No such signal is conclusively detected in the more rapidly orbiting systems studied.

**Key words:** stars - X-rays: binaries :pulsars

## 1 INTRODUCTION

The Burst And Transient Source Experiment on the Compton Gamma Ray Observatory (Fishman et al 1989) provided near continuous monitoring of the whole sky at hard X-ray energies. BATSE only sees the high energy tail of HMXBs, typically detected in the lowest DISCLA channel and CONT channels 1-4 covering 20-70keV. In studying X-ray pulsars two modes of operation are possible; pulsed flux and Earth occultation. If pulsations are detected corresponding to the spin period of a known pulsar then the pulsed flux and pulse frequency can be measured with Fourier analysis or epoch folding (Bildsten, L. et al. 1997) and used to monitor the source with great sensitivity and fine time resolution. (Bildsten et al 1997) For the long term study of behavior related to orbital motion in binary systems, daily averages of the total flux are sufficient and are in addition sensitive to non-pulsed X-ray output from the source. By exploiting the Earth's limb as an occulting mask, individual X-ray sources can be isolated with an accuracy of  $1^\circ$ . Termed the Earth Occultation Technique, two measurements of the total flux

from a source are made during each 90 minute satellite orbit as the source moves into and out of eclipse due to the satellite's motion, full details are given by Zhang et al ( 1994) & Harmon et al ( 2002).

In this paper we present folded X-ray lightcurves of Type I (normal) outbursts from 8 HMXBs in which periodic fluctuations corresponding to previously published orbital periods were significantly detected. Such outbursts are thought to occur at each periastron passage of the neutron star. These outbursts last for 8-10 days and the X-ray luminosity increases by a factor of  $\sim 10$ . In contrast, Type II are giant outbursts which do not correlate with the orbital phase but tend to last for several orbital cycles. The X-ray luminosity during the outburst may reach close to the Edington luminosity.

In addition we studied the 30.5d modulation from LMC X-4 which was also a significant detection and investigated the X-ray behaviour of A0538-668 in the light of recent optical work (Alcock et al 1999). The BATSE datasets for these systems cover many orbital cycles and hence present the first ever opportunity to study their long term behavior. Previ-

ously only widely spaced, scheduled or chance observations were available for this purpose. Usually made with different instruments having little or no overlap in terms of spectral response, extrapolating long term trends from previous data was of limited value.

The publicly available pulsed flux monitor reports produced by MSFC demonstrates that HMXBs typically exhibit active epochs lasting several months interspersed with quiescent periods. A question we addressed was that of possible changes in behaviour between these epochs. If a source is bright enough or its active epochs span enough orbital cycles then folded X-ray lightcurves from different epochs can be directly compared and variations in behavior detected.

Variability in the X-ray recurrence period can be looked for in the power spectrum of the flux history. Width of the recurrence frequency peak will be increased if that frequency varies, in other words if the exact time at which the outbursts turn on varies from orbit to orbit then this will show up in the power spectrum. If such jitter can be identified this could provide clues about the underlying physical behaviour of such systems. For example theory indicates that accretion rates are effected by a neutron star's speed relative to its surroundings. The Alfvén speed in stellar wind plasma is a function of both magnetic field strength and plasma density. Thus a high outflow velocity of a wind or circumstellar disk may inhibit accretion during periastron passage and push the X-ray outburst to a later phase. Additionally the orientation of the magnetic field frozen into a plasma strongly affects its coupling to a magnetosphere moving through it. These effects, although extremely difficult to measure directly, may leave a signature in possible chaotic fluctuations or jitter in the exact phase at which outbursts turn on. The jitter is expected to be chaotic because there is no direct connection between the plasma properties and the binary motion, yet the stability of the accretion disk depends on a dynamic balance between accretion rate onto the disk and accretion rate onto the neutron star.

Secondary outbursts occurring close to apastron of the neutron star are also a key observation in this study. Their existence and exact phase at which they occur will yield information about circumstellar disk outflow and stellar wind parameters, principally outflow velocity and density information. Higher outflow velocity is expected to delay periastron outburst turn-on and is cited as a possible cause of apastron outburst in the Bondi-Hoyle theory of accretion. Our folded lightcurves show that EXO2030+375, GX301-2 and 4U1145-619 may exhibit X-ray emission at apastron passage of the neutron star. Whether this emission occurs always or only sporadically, is impossible to determine from individual orbits, so long-term coverage is a necessity.

In these preliminary interpretations of our lightcurves we are aware that BATSE only sees the high energy tails of the emitted X-ray spectra of these sources. Lightcurve shape is thus affected by the true spectral profile of the emitted X-rays and the spectral response of the detector. The most significant effect is expected to occur at the peak of periastron outbursts, when there is the highest column density of obscuring matter and the most intense flux of hard photons, leading to X-ray reprocessing and re-radiation at lower energies.

Parameters for the 8 systems studied are shown in Table 1. Of these sources, in all cases but LMC X-4 the modulation

studied is directly linked to orbital motion. In LMC X-4 the binary period of 1.4d is not seen because it is too faint in hard X-rays. The 1.4 day orbital period of LMC X-4 is above the Nyquist limit for this data (about 2.4d) so aliasing will shift this frequency in the power spectrum, but no significant signal is detected. However the well known periodicity near 30.5 days was detected and a lightcurve constructed. An improved measurement was made of X-ray modulation due to the precession of a warped accretion disk.

Note that throughout this paper dates are presented as Truncated Julian Dates (TJD), where  $TJD = JD - 2440000.5$ .

## 2 DATA PROCESSING AND DATA ARTEFACTS

The BATSE dataset used in this work consists of daily averages of the flux levels derived from the occultation technique at MSFC (Harmon et al 2002).

In the occultation technique, source fluxes are in principle measured twice every spacecraft orbit, as rising and setting steps. However, in practice, not all occultation steps are available for measurement. The most common reason steps are unavailable are (1) passage of the spacecraft through the lower Van Allen radiation belt at the South Atlantic Anomaly, when the detector high voltage was turned off; (2) periods of time when CGRO was out of line-of-sight contact with the NASA Tracking and Relay Satellites (TDRS); and (3) data which were flagged by the BATSE operations team (i.e. during gamma ray bursts, solar flares, etc.) and were not available for analysis. The oblateness of the Earth causes the CGRO orbit to precess with a period of about 53 days. During the precession cycle, high declination sources ( $|\delta| \geq 41^\circ$ ) cease occulting near the orbital poles.

When occultation steps are measured, the background is estimated using 110 seconds of data before and after the occultation step, called the fitting window. Occultation steps from sources other than the measured source within this window are considered interfering sources. If occultation steps of an interfering source occur within 10 seconds of the measured source, that step is discarded. The number of interfering sources in the fit affects the systematic error in three ways (1) where sharing of flux occurs between source terms in the fitting process and (2) where sources are either included or not included in the fit because of an incorrect assumption about the sources' relative intensity to the measured source or (3) when an unknown source is present in the fitting window. Other sources of systematic error include red noise and coherent pulses from bright X-ray sources present, but not necessarily occulting, within the fitting window.

To estimate the average systematic error, a grid covering the galactic plane with points every 3 degrees along the galactic plane with two additional sets of grid points at +6 degrees and -6 degrees galactic latitude. Grid points within 2 degrees of bright occultation sources were excluded, yielding a total sample of 156 points. The average flux from each grid point was averaged over a 9 year period and the standard deviation of 1-day flux averages was computed as a function of galactic longitude. The values for the standard deviations are larger than expected for a Gaussian distribution about zero flux due to various systematic effects. We

find broadening factors of about 30%-60% in excess of normal statistics, strongest near the galactic center and near bright variable sources such as Vela X-1 and Cygnus X-1. Both positive and negative trends are present in the average fluxes. For example, near EXO2030+375 ( $l_{II} = 77.2$  degrees,  $b_{II} = -1.3$  degrees), the average flux at  $b_{II} = 0$  degrees is 0.0077, 0.0009, -0.001 photons  $\text{cm}^{-2}\text{s}^{-1}$  and standard deviation 1.85, 1.42, 1.26 (1 sigma = 0.01 photons  $\text{cm}^{-2}\text{s}^{-1}$ ) for longitudes  $l_{II} = 72.0, 78.0,$  and  $84.0$  degrees, respectively (Harmon, B.A. et al. 2002). Clearly interfering sources in various regions of the sky produce both positive and negative offsets in flux. These fluxes may be modulated at the precession period and may change sign, depending on the limb geometry.

Data gaps arise due to three specific causes: passage through the South Atlantic Anomaly when the detectors are switched off; known interfering source occulting within 10 seconds of the target; periods when the source is occulted by the earth's limb at too shallow an angle for a significant detection to be made (or is not occulted at all). The latter effect happens only for sources lying at greater than 41 degrees in declination.

Interfering sources that are positively identified should be fitted for in the occultation technique, however this is (as in the case of the background correction) a question of optimisation and so interfering sources are not always completely removed. A signature of source interference is significant negative flux indicating that a persistent source close to the target has not been fitted correctly in calculating the occultation step-height for the target source. Provided the interfering source has not varied on timescales comparable to the recurrence period of the target, it will be averaged out in the epoch folding procedure. If however the source has varied then its effects must be positively identified before a folded lightcurve can be produced.

Unidentified sources of interference pose an additional problem in that their position relative to the earth's limb and the target change continuously. This leads to modulation at the precession period as the interference contribution varies cyclically with the orbital plane. This type of artefact may be non sinusoidal although subtracting a sinewave with correct period and amplitude can attenuate it in some cases. In principle such signals could be used iteratively to improve the occultation analysis but this is not practical at this time. Persistent and identified transient sources of interference can be investigated on a source by source basis. In some cases datapoints or stretches of data have to be excluded, if for example a nearby source flares unpredictably. While in some datasets the interference is clearly apparent as a completely distinct feature in the power spectrum and can be attenuated by subtracting a sinewave fit to the modulation if necessary. Scargle (1989) states that the modified power spectrum (Lomb-Scargle periodogram) is equivalent to least-squares fitting with sinewaves, hence our procedure is equivalent to filtering the data in the frequency domain.

## 2.1 Implications of uneven sampling

Unevenly sampled data cannot be correctly analysed by the direct Fourier Transform technique as the resulting power spectrum is a convolution of both the source frequencies and sampling frequencies. This leads to spurious frequencies

and possible suppression of genuine signals. Specifically; uneven sampling increases leakage of power to nearby frequencies, although at the same time, aliasing may be reduced. Our data are very unevenly sampled, especially when we excluded subsets of the data e.g. data intervals selected on the basis of an ephemeris in order to search for the possible 16.65d transient modulation in A0538-668. Fortunately the Lomb-Scargle periodogram is formulated for exactly this situation and is relatively insensitive to the sampling structure (Scargle 1982, 1989).

A further complication is the non-sinusoidal nature of many of the lightcurves, generally the less sinusoidal a signal is, the more components it will have in any frequency space representation. These components are seen in power spectra as sidebands to the main frequency spike. If the shape of an otherwise regular modulation changes with time, these peaks can become broadened, shift and become blended together. Thus in our period determinations we backed up the Lomb-Scargle result with Phase Dispersion Minimisation analysis (PDM). (Stellingwerf 1978). Such periodograms typically contain a number of local minima corresponding to (For example) integer multiples of the true period. However the PDM technique is totally insensitive to the shape of the lightcurve and this makes for highly accurate period determinations in the case of irregular lightcurves. Periods were measured from the PDM periodogram by calculating the centroid of the feature of interest. We relied on the Lomb-Scargle periodogram for our primary detection tool because the separation of Fourier components is better suited to identification of interfering sources, sidebands, aliasing and statistical modeling of the signal. PDM was implemented in the Starlink program 'Period'.

## 2.2 Evaluation of signal detection confidence levels

In detecting weak, unevenly sampled, periodic signals against a varying background, statistical significance is a key issue. The only reliable way to evaluate the confidence levels associated with a power spectrum under these conditions is by statistical simulation.

We first measured the mean and variance of each dataset, we then created a series of random numbers conforming to a Gaussian distribution with the same mean and variance as each dataset. This series was then combined with the sampling structure (Timing information) of the original dataset by simply replacing each flux measurement with a number drawn from the random gaussian distribution. Thus creating a simulation of what BATSE might have seen, had there been no periodic X-ray sources in its field of view. This dataset was then subjected to Lomb-Scargle analysis and the power of the highest peak and the highest peak in a specified frequency range recorded. This process was then repeated 1000 times after which the mean and variance of the peak noise power (PNP) were calculated, both for the whole spectral range available and for the specified frequency range of interest. For the Lomb-Scargle periodograms presented here, the displayed confidence levels are the mean PNP + 3 standard deviations. Thus our confidence levels directly reflect how likely it is that a given signal is real or due to chance without making any assumptions about the underlying properties of the data. The confidence levels calculated

**Table 1.** Summary of the observational parameters of HMXRBs studies in this work. A0538-668 is not included in the table because it was not detected in the BATSE data sample. TJD = Julian date - 2440000.5. For EXO2030+375 epoch 1 corresponds to TJD8363.5 - 9353.5 and epoch 2 to TJD10114.5 - 10723.4. Column 4 gives the epoch of periastron passage used (Bildsten et al 1997), except in the case of 4U1145-619 and 4U1700-377 which are arbitrary dates. The last two columns compare the observed peak in the Lomb-Scargle power spectrum with Monte Carlo simulated data - see text for details.

X-ray Source	Optical Counterpart	Orbital period (days)	T <sub>0</sub> (TJD)	Detection Significance	BATSE data Peak FWHM $\times 10^{-4} d^{-1}$	Simulated data Peak FWHM $\times 10^{-4} d^{-1}$
EXO2030+375 epoch 1	Be	46.01	8936.50	33.3 $\sigma$	8.70	9.06 $\pm$ 0.34
EXO2030+375 epoch 2	Be	46.01	8936.50	3.47 $\sigma$	16.4	15.6 $\pm$ 6.0
4U1145-619	Be	186.5	8363.51	5.68 $\sigma$	4.56	3.72 $\pm$ 1.7
4U1700-377	SG	3.412	8363.54	241 $\sigma$	3.50	3.40 $\pm$ 0.06
4U1907+097	SG	8.38	5578.75	3.41 $\sigma$	4.86	3.61 $\pm$ 2.0
Cen X-3		2.087	8561.50	29.7 $\sigma$	3.27	3.44 $\pm$ 0.13
GX301-2	SG	41.5	8802.79	139 $\sigma$	3.65	3.45 $\pm$ 0.09
LMC-X4	Be	1.4, 30.35	7741.99	86.0 $\sigma$	3.34	3.46 $\pm$ 0.10
OA01657-41	SG	10.44	8515.99	74.5 $\sigma$	3.26	3.41 $\pm$ 0.09

by this procedure for each dataset were later used in evaluating the Lomb-Scargle periodograms generated from simulated datasets.

### 2.3 Jitter in outburst turn-on times

The width (FWHM) of peaks in the power spectrum may be related to orbit-to-orbit variation in the exact time at which outbursts occur. We investigated this by comparing the FWHM of the orbital modulation peak in the Lomb-Scargle periodogram to that measured for a simulated dataset containing a sinewave of appropriate period and amplitude superimposed on a background created by randomizing the flux readings in the original dataset. Results are shown in Table 1 for comparison. Further investigation of this parameter by a Monte-Carlo technique showed that the FWHM is dependent on the noise present. Specifically the FWHM becomes more variable as the S/N ratio deteriorates. Combined with the well known dependence of the FWHM on the length of the dataset, the resolution of the periodogram in respect of this parameter had to be calculated independently for each dataset. For each source a Monte-Carlo simulation was run by first finding the correct amplitude sinewave to give the same S/N ratio as that seen in the data -using the limit finding procedure described in section 3.1.1. The flux values in the data were then repeatedly randomized and added to this signal. The Lomb-Scargle periodogram was calculated each time and the FWHM of the peak measured and recorded. After 100 cycles the mean and standard deviation of the FWHM were calculated and the results are displayed in Table 1.

In addition to movement in the outburst phase it is possible that other effects such as variations in the shape of the outburst profile might also give rise to a widening of the peak in the power spectrum. However, inspection of the results presented in Table 1 shows no evidence of any variability in the power spectrum peak indicating a general lack of jitter in turn-on times and no significant variation in the outburst profiles.

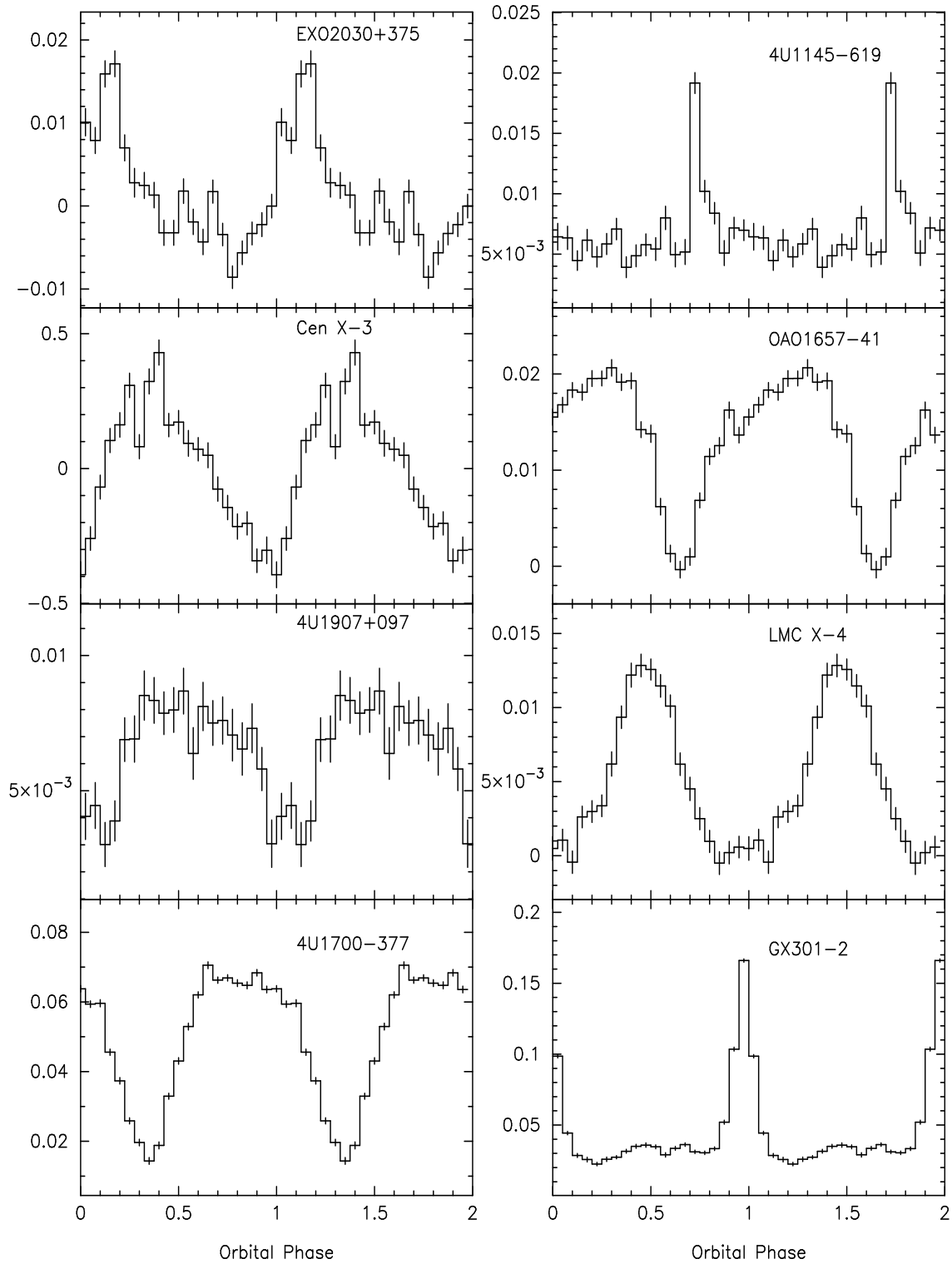
## 3 RESULTS

Table 1 summarises key observational parameters of the HMXBs studied, while Figure 1 shows the X-ray lightcurves folded over 20 phase-bins. The errors shown are observational errors inherent in the occultation analysis, in producing the averaged lightcurves, the error-bars are the standard deviation of points in each phase-bin.

### 3.1 Link between Type I X-ray outbursts and long period optical variations in A0538-668

We tested the prediction that A0538-668 only exhibits X-ray outbursts correlated with its orbital period at times coincident with minima in its long period optical lightcurve. (Alcock et al 1999) We note that previous widely spaced X-ray observations of A0538-668 tend to support this hypothesis, however we find conclusively that between TJD 8363 - 10999 (The time span of the BATSE occultation data) no significant modulation of 20-70 keV X-ray flux at the orbital period is present at the predicted epochs. To do this we calculated an ephemeris for precise times at which this model predicts outbursts to occur. The orbital parameters were taken from Skinner ( 1982), P=16.65d, with a zero-point T<sub>0</sub>=TJD 3423.96 Maxima are expected at phase 0.9 in this scheme if the X-rays follow the optical variability. The long period parameters from Alcock et al ( 1999) are under this scheme: P=420.82d, with arbitrary zero-point TJD 9001. The long period minima occur at arbitrary phase 0.55. The ephemeris was then used to isolate time intervals when X-ray outbursts were expected. The duration of the time interval examined either side of long period minima was 100 days to cover the data coincident with the optical lightcurve "dip" regions.

According to Skinner ( 1982), A0538-668 was in the field of view of the Einstein satellite on four occasions. According to the ephemeris described here, detections reported on 16 Dec 1980 and 3 Feb 1981 lie in the optical dip, and non detections on 10 Apr 1979 and 30 May 1980 lie firmly in the centre of the bright phase of the optical lightcurve.



**Figure 1.** Phase-averaged lightcurves created from BATSE occultation flux measurements. All data are folded at the periods and phases given in Table 1 except for 4U1907+09 which is folded at twice the period quoted in the table (see text for details).

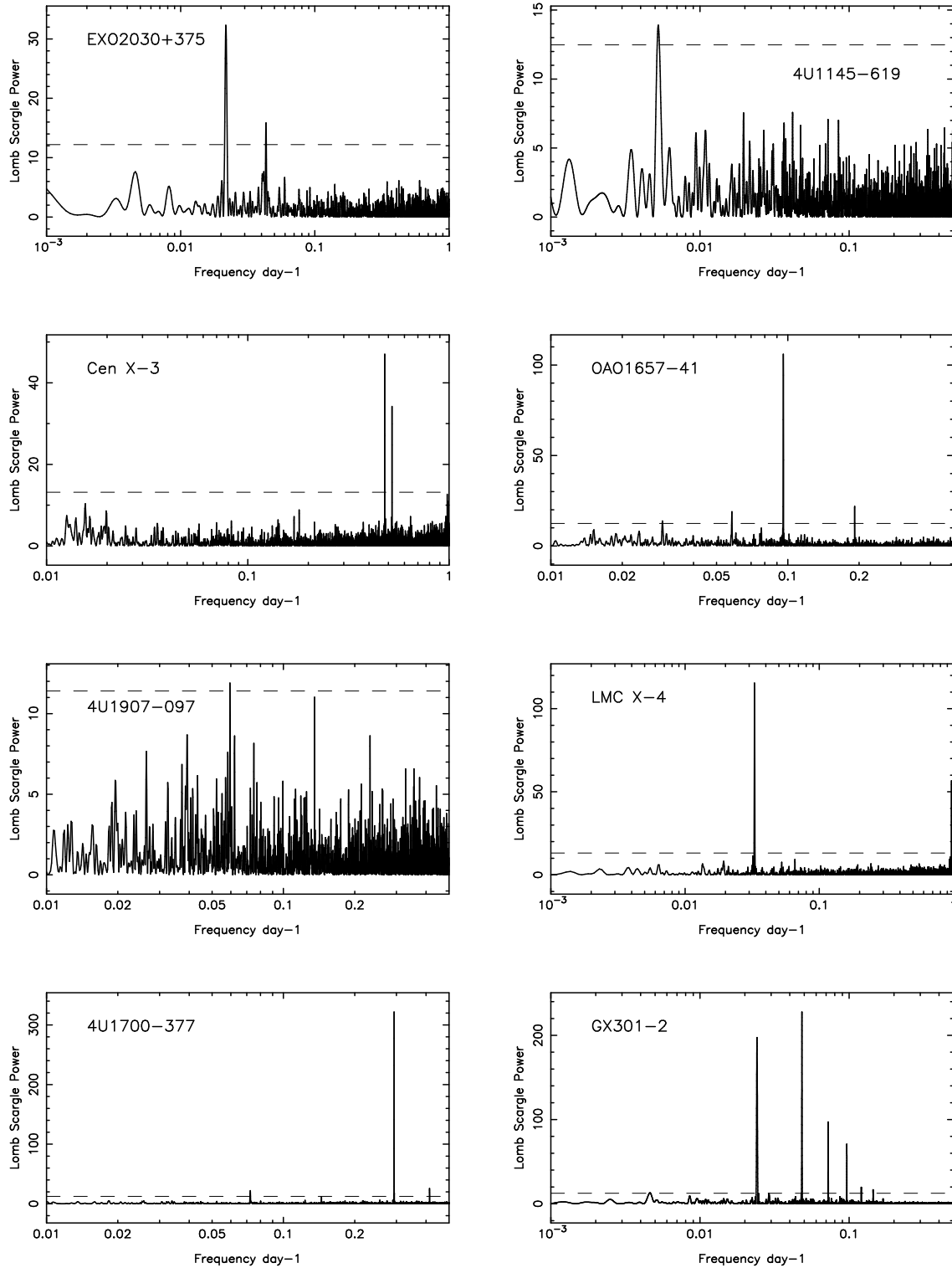


**Figure 2.** Lomb-Scargle periodograms of BATSE occultation flux histories. The  $3\sigma$  significance levels are plotted as dashed lines. These levels are calculated by Monte-Carlo simulations over the frequency space displayed (see Section 2.2).

### 3.1.1 BATSE detection threshold for A0538-668

By creating test datasets with the same mean and variance as the BATSE data and containing only simulated signals, we determined how strong a periodic signal must be in order to give a  $3\sigma$  detection. This approach could also be used to model other components of a power spectrum, particularly where interfering sources and sampling structure lead to spurious frequencies.

Known interfering signals in the A0538-668 data include LMC X-4 (which is only  $0.6^\circ$  away and dominates the periodic flux in this dataset) and the spacecraft precessional modulation. These components were modelled by measuring their amplitudes in folded lightcurves at 35.5d and 52d respectively.

Using the ephemeris described above BATSE data were selected which were coincident with the four long-period optical minima observed during the MACHO observations of Alcock et al (1999). This resulted in four blocks of BATSE one-day averages each of duration 100 days spanning the time interval TJD 9124.52 - TJD 10999.5. Having failed to detect any statistically significant modulation consistent with 16.65 days, this subset of the BATSE observations of A0538-668 was then repeatedly randomized to destroy any periodic content and combined with an incrementally increasing sinusoidal signal plus fixed sinewave components to simulate the interfering sources in the real data. After each step, the Lomb-Scargle periodogram was computed and the highest peak in a pre-determined frequency range was compared to the  $3\sigma$  confidence level previously calculated for that frequency range as described in section 2.3. Once this threshold was exceeded, the amplitude of the sine wave signal was recorded. The detectability of such a weak signal is somewhat influenced by the noise present. At the very margins of detectability the power in a given frequency can fluctuate up and down despite a gradual increase in signal amplitude. Hence we used the criterion that the power in the selected frequency range must remain above the threshold value irrespective of chance structures in noise in order to qualify. The derived upper limit was independently tested using many different noise sets to verify this criterion was met, i.e. That a signal of the amplitude quoted would definitely have been detected by the methods described here, had it been present. Weaker signals would not consistently rise above the threshold although detections of marginal significance are possible.

## 4 DISCUSSION

### 4.1 EXO2030+375

This object has been subject of several recent studies. Reig et al (1998) presented results of multi-wavelength observations and modeling of the accretion rate. Wilson et al (2002) report on a decade of X-ray observations combined with IR and H $\alpha$  measurements which show a decline in the density of the circumstellar disk around the Be star. This decline was followed by a sudden drop in the X-ray flux and a turn-over from a spin-up trend to spin-down in the frequency history. This is the first Be/X-ray binary to show an extended interval, about 2.5 years, where the global trend is spin-down, but the outbursts continue. In 1995 the orbital phase of EXO

2030+375's outbursts shifted from peaking about 6 days after periastron to peaking before periastron. The outburst phase slowly recovered to peaking at about 2.5 days after periastron. Wilson et al (2002) interpret this shift in orbital phase followed by a slow recovery as evidence for a global one-armed oscillation propagating in the Be disk. This was further supported by changes in the shape of the H $\alpha$  profile which are commonly believed to be produced by a reconfiguration of the Be disk. The truncated viscous decretion disk model provided an explanation for the long series of normal outbursts and the evidence for an accretion disk in the brighter normal outbursts.

In the present analysis we find convincing evidence for elevated flux levels at apastron in the earlier epoch (see Figure 1). The RXTE ASM lightcurve for epoch 2 was studied by Reig et al (1998), we also analysed this data in order to compare the lightcurve and power spectrum with the BATSE results. The power spectra from both instruments appear to share the same features in epochs 1 & 2, peaks at  $P_{orb}$  &  $P_{orb}/2$  with powers at similar ratios. Direct comparison of the BATSE and RXTE folded lightcurves suggests that X-ray emission from EXO2030+375 may be softer during the apastron outbursts than during the normal Type I outbursts at periastron. This hypothesis is drawn from the relative amplitudes of the two peaks in the lightcurve and the differing spectral responses of the two instruments.

Comparison of the FWHM of the orbital period peak at 46d with that derived from simulated data reveals that although the phase of peak outburst intensity shifts between the two epochs, its recurrence is otherwise periodic. There is no evidence for any gradual shift in phase in either epoch.

### 4.2 A0538-668

We find that during the period coincident with the MACHO monitoring of Alcock et al (1999), A0538-668 did not exhibit hard X-ray outbursts at the 16.65 day orbital period during either the optical minima or maxima. The upper limit for such activity is found to be  $3.0 \times 10^{-3}$  photon  $\text{cm}^{-2} \text{s}^{-1}$  at 20-70 keV. We compare this limit with the X-ray spectrum obtained with Ariel V (White & Carpenter 1978) at the peak of the July 1977 outburst. By assuming a mean photon energy of 45 keV over a spectral range of 20-70 keV for the BATSE observations we estimate a maximum flux density of  $2.7 \times 10^{-3} \text{ keV cm}^{-2} \text{ s}^{-1} \text{ keV}^{-1}$ . The fitted spectrum of White & Carpenter (1978) is extremely steep and dominated by a thermal component. By extrapolating their model, our lower limit for detection by BATSE in the data presented here is consistent with the flux that would be expected on the basis of this model to within errors. Thus we conclude that had A0538-668 been active at its previous level BATSE would have detected it.

### 4.3 Centaurus X-3

This source was detected in BATSE data at  $29\sigma$  with a period 2.087d. Cen X-3 is the only HMXB to have a well determined orbital period derivative (Nagase et al 1992) however this is too small to show up in our analysis. The power spectrum in Figure 2 shows two peaks, but comparison with the power spectrum for simulated data showed

the higher-frequency peak to be an artefact of aliasing. The folded lightcurve Figure 1 is a simple sawtooth like form, brightening more rapidly than it decays.

#### 4.4 4U1907+097

Two peaks with  $\sim 3\sigma$  significance are found at periods of 16.8d and 7.39d. The orbital period of the system is believed to be 8.38d (Marshall and Ricketts 1980, Cook and Page 1987) thus the 16.8d X-ray modulation is consistent with twice the binary period. However, there is no evidence for a peak in the power spectrum at  $\sim 8.4$ d - this is not surprising if one considers the folded lightcurve in Figure 1 which shows just a single broad peak when folded at 16.8d. Constructing a simulated dataset containing a sinewave at 8.38d with amplitude taken as 0.002 (measured from a lightcurve folded at this period) failed to reproduce the 16.8d modulation. Thus it appears that the emission is really modulated at twice the binary period in these BATSE data.

#### 4.5 4U1700-377

Early BATSE occultation data from this source have already been the subject of a paper by Rubin et al., 1996. Our PDM period agrees with  $3.41180 \pm 0.00003$ d from Copernicus X-ray observation (Braduardi 1978). We also detect significant peaks in the power spectrum at 13.808d at a significance of  $11.3\sigma$ , and at exactly half this period. This period has been previously reported by König & Maisack (1997). We further investigated this period by subtracting the orbital modulation from the lightcurve, using Figure 1 as a template. This procedure resulted in reduction of spectral power at the orbital period by a factor of 24. No attenuation of the 13.808d period was observed, in fact a significant increase resulted. Hence we are confident that the 13.808d period is an independent modulation and not an harmonic of the orbital period.

#### 4.6 4U1145-619

A peak was detected in LS periodogram at 190.238d with FWHM=17.48 days. A PDM periodogram determination of  $186.6 \pm 0.348068$ d measured by centroiding is consistent with the established value of 186.5 days.

#### 4.7 OAO1657-41

The PDM period of  $10.4626 \pm 0.0011$ d is in agreement with the period of  $10.4436 \pm 0.0038$ d (Chakrabarty et al 1993) from BATSE pulse timing studies.

#### 4.8 LMC X-4

The 1.4d binary period is not detected. The "average" Nyquist period of the daily average data is 2.4d so the single-step data was also analysed, again with no detection. The 30.5d X-ray modulation believed to be due to the precession of a warped accretion disk (Lang et al 1981) is detected and is shown to be persistent throughout the full span of the data Figure 1. All period finding techniques tried, (Lomb-Scargle, PDM, CLEAN) derive a period for this modulation

slightly shorter than usually quoted. A PDM periodogram constructed at a resolution of  $2 \times 10^{-5}$  cycles and measured by centroiding, derived a period of 30.349d while the L-S periodogram yielded 30.355d. Monte Carlo simulations of sinusoidal signals at 30.5d and 30.35d superimposed on noise created by randomizing the original dataset show that the LS periodogram frequency resolution is  $1.43765 \times 10^{-5}$  at the S/N level seen in the data. A solution at 30.5d is thus seemingly in conflict with the BATSE dataset. A remarkable fact is the stability of this modulation over the 7 years of data, since no jitter is evident from the values in Table 1

#### 4.9 GX301-2

This system is clearly the brightest, most regular source studied here. The phase-binned folded lightcurve shows increasing flux levels consistent with phase 0.5, each of which reached type-I outburst levels. This result confirms previous work by Pravdo et al, 1995 and Koh et al, 1997 - both of these works also present evidence for apastron outbursts from this system. The power spectrum for GX301-2 shows a pattern of strong peaks which after comparison to simulated data are found to be real. These frequency components, appearing at integer submultiples of the orbital period are a signature of the highly non-sinusoidal lightcurve. The spectrum shown is that generated after the removal of 4 particularly bright apastron flux points, as expected their inclusion boosts the  $P_{orb}/2$  component.

## 5 CONCLUSIONS

Observations of accreting pulsars in high mass binary systems using the BATSE occultation technique reveal that this approach is sufficiently sensitive to derive accurate measurements of the X-ray modulation. Evidence for apastron X-ray outbursts is found in 2 sources: EXO2030+375 and 4U1145-619. All of these sources are in high mass, long period systems, EXO2030+375 and 4U1145-619 have similarities in their folded lightcurves having flux levels significantly above minimum for most of each orbit and apastron features reaching 30-40 percent of peak flux. GX301-2 has a much flatter minimum level between emissions and the apastron emission is only 10 percent of peak flux. These differences undoubtedly reflect the different nature of the companion star, whether Be or supergiant. The fact that none of the shorter period systems show evidence for this phenomenon may be explainable in terms of the standard Bondi-Hoyle accretion model if suitable parameters can be estimated/calculated for the outflow velocity and density of the circumstellar material/wind along the orbital trajectory of the neutron star. We hypothesise that in short period systems the radial profile of the stellar wind can never satisfy the required conditions for apastron outbursts due to the smaller apastron separation distances and higher neutron star velocities involved. The FWHM of the orbital period peaks in the power spectra were investigated as a possible indicator of variability in the exact time at which outbursts "switch on". To within the uncertainties imposed by the signal/noise ratio of the data this effect was not detected in any of the sources.

## ACKNOWLEDGMENTS

SL acknowledges the use of STARLINK software and the support of a PPARC studentship.

## REFERENCES

- Alcock C., Allsman R. A., Alves D. R., Axelrod T. S., Becker A. C., Bennett D. P., Charles P. A., Cook K. H., Drake A. J., Freeman K. C., Griest K., Lehner M. J., Marshall S. L., McGowan K. E., Minniti D., Peterson B. A., Pratt M. R., Nelson C. A., Quinn P. J., Stubbs C. W., Sutherland W., Tomaney A. B., Vandehei T., Welch D. L., 1999, MNRAS, (in press)
- Bildsten L., Chakrabarty D., Chiu J., Finger M. H., Koh T., Nelson R. W., Prince T. A., Rubin B. C., Scott D. M., Stollberg M., Vaughan B. A., Wilson C. A., Wilson R. B., 1997, ApJS, 113, 367.
- Branduardi G., Mason K. O., Sanford P. W., 1978, MNRAS 185, 137
- Chakrabarty D., Grunsfield J. M., Prince T. A., Bildsten L., Finger M. H., Wilson R. B., Fishman G. J., Meegan C. A., 1993, ApJ, 403, L33
- Chakrabarty et al, ApJ 446:826, 1995
- Charles P. A., Smale ., 1986, ApJ 305,814
- Cook M.C. & Page C.G., 1987, MNRAS, 225, 381.
- Fishman et al, Proc. GRO Science Workshop, ed W. N. Johnson., NASA pub., 2-39
- Harmon B. A., Fishman G. J., Wilson C. A., Paciasas W. S., Zhang S. N., Finger M. H., Koshut T. M., McCollough M. L., Robinson C. R., Rubin B. C., 2002, ApJS, 138, 149.
- Koh, D. T., Bildsten, L., Chakrabarty, D., Nelson, R. W., Prince, T. A., Vaughan, B. A., Finger, M. H., Wilson, Robert B., Rubin, Bradley C., 1997, ApJ 479, 933.
- Konig M. & Maisack M., 1997, A&A, 327, L33.
- Marshall N. & Ricketts M.J., 1980, MNRAS, 193, 7p.
- Lang F. L., Levine A. M., Bautz M., Hauskins S., Howe S., Primini F. A., Lewin w. h. G., Baity W. A., Knight F. K., Rothschild R. E., Petterson J. A., 1981 ApJ 246, L21
- Nagase F., Corbet R. H. D., Day C. S. R., Inoue H., Takeshima T., Yoshida K., 1992, ApJ 396, 147-160
- Pravdo, S.H., Day, C. S. R., Angelini, L., Harmon, B. Aa, Yoshida, A., Saraswat, P., 1995, ApJ 454, 872.
- Reig P., Stevens J. B., Coe M. J., Fabregat J., 1998, MNRAS, 301, 42
- Rubin, B. C., Finger, M. H., Harmon, B. A., Paciasas, W. S., Fishman, G. J., Wilson, R. B., Wilson, C. A., Brock, M. N., Briggs, M. S., Pendleton, G. N., Cominsky, L. R., Roberts, M. S. 1996, ApJ, 459, 259.
- Scargle J. D., 1982, ApJ 263,835
- Scargle J. D., 1989, ApJ 343,874-887
- Skinner G. K., Bedford D. K., Eisner R. F., Leahy D., Weisskopf M. C., Grindlay J., 1982 Nature, 297, 5867
- Stellingwerf R. F., 1978 ApJ 224, 953
- Warwick et al. 1989, Space Sci. Rev. 40, 429
- White N. E., Carpenter G. F., 1978, MNRAS 183,11p-15p
- Wilson C.A., Finger M.H., Coe M.J., Laycock S.G.T., Fabregat J. 2002 ApJ (in press)
- Zhang et al., 1994, IEEE Trans. Nuclear Sci. vol. 41, No.4